



HAL
open science

Inhibition of ice crystallisation in highly viscous aqueous organic acid droplets

B. J. Murray

► **To cite this version:**

B. J. Murray. Inhibition of ice crystallisation in highly viscous aqueous organic acid droplets. Atmospheric Chemistry and Physics Discussions, 2008, 8 (3), pp.8743-8771. hal-00304158

HAL Id: hal-00304158

<https://hal.science/hal-00304158>

Submitted on 18 Jun 2008

HAL is a multi-disciplinary open access archive for the deposit and dissemination of scientific research documents, whether they are published or not. The documents may come from teaching and research institutions in France or abroad, or from public or private research centers.

L'archive ouverte pluridisciplinaire **HAL**, est destinée au dépôt et à la diffusion de documents scientifiques de niveau recherche, publiés ou non, émanant des établissements d'enseignement et de recherche français ou étrangers, des laboratoires publics ou privés.

**Inhibition of ice
crystallisation**

B. J. Murray

Inhibition of ice crystallisation in highly viscous aqueous organic acid droplets

B. J. Murray

School of Chemistry, Woodhouse Lane, University of Leeds, Leeds LS2 9JT, UK

Received: 28 March 2008 – Accepted: 3 April 2008 – Published: 14 May 2008

Correspondence to: B. J. Murray (b.j.murray@leeds.ac.uk)

Published by Copernicus Publications on behalf of the European Geosciences Union.

Title Page

Abstract

Introduction

Conclusions

References

Tables

Figures

◀

▶

◀

▶

Back

Close

Full Screen / Esc

Printer-friendly Version

Interactive Discussion



Abstract

Homogeneous nucleation of ice within aqueous solution droplets and their subsequent crystallisation is thought to play a significant role in upper tropospheric ice cloud formation. It is normally assumed that homogeneous nucleation will take place at a threshold supersaturation, irrespective of the identity of the solute, and that rapid growth of ice particles will follow immediately after nucleation. However, it is shown here through laboratory experiments that droplets may not readily freeze in the very cold tropical tropopause layer (TTL, typical temperatures of 186–200 K). In these experiments ice crystal growth in citric acid solution droplets did not occur when ice nucleated below 197 ± 6 K. Citric acid, 2-hydroxypropane-1,2,3-tricarboxylic acid, is a molecule with similar functionality to oxygenated organic compounds which are ubiquitous to atmospheric aerosol and is therefore thought to be a sensible proxy for atmospheric organic material. Evidence is presented that suggest citric acid solution droplets become ultra-viscous or perhaps even glassy under atmospherically relevant conditions. Diffusion of liquid water molecules to ice nuclei is expected to be very slow in ultra-viscous solution droplets and this most likely provides an explanation for the experimentally observed inhibition of ice crystallisation. The implications of ultra-viscous solution droplets for ice cloud formation and supersaturations in the TTL are discussed.

1 Introduction

Ice clouds that form in the Earth's upper troposphere (UT) are known to play a significant role in the planet's radiation budget and climate (Liou, 1986), but mankind's impact on these clouds is uncertain (Denman et al., 2007). Ice clouds in the UT also influence the entry of water vapour into the stratosphere by acting as a cold trap (Jensen and Pfister, 2005), and they provide a surface on which chemical species may adsorb and react (Abbatt, 2003). A quantitative knowledge of the fundamental ice nucleation and crystallisation processes of these clouds is essential in order to understand and predict

Inhibition of ice crystallisation

B. J. Murray

Title Page

Abstract

Introduction

Conclusions

References

Tables

Figures

◀

▶

◀

▶

Back

Close

Full Screen / Esc

Printer-friendly Version

Interactive Discussion



their impact on the Earth's atmosphere and climate.

An important mechanism of UT ice cloud formation is through the homogeneous freezing of aqueous solution droplets. Homogeneous freezing is a multi-step process, which begins with nucleation of ice which then triggers ice crystal growth and the resulting aqueous brine may also crystallise to form a crystalline solute phase or phases (Murray and Bertram, 2008). Ice crystal growth may then continue by deposition from the vapour phase until the water vapour supersaturation is relaxed and ice particles exits in equilibrium with the surrounding atmosphere. In a landmark paper, Koop et al. (2000) showed that homogeneous nucleation in aqueous solution droplets only depends on water activity (a_w) for a wide range of solution droplets. The water activity of droplets at equilibrium equals the relative humidity (with respect to liquid water, RH_w) of the surrounding atmosphere (i.e. $a_w = RH_w/100$, at equilibrium). Hence the homogeneous freezing threshold can be defined in terms of RH_w ; this greatly simplified the description of homogeneous freezing in cloud formation models. However, recent observations of very high supersaturations both in and out of very cold ice clouds in the tropical tropopause layer (TTL, ~ 11 – 18 km, typically ~ 185 – 200 K, Gettelman and Forster, 2002) have brought into question our fundamental understanding of cold ice cloud formation (Jensen et al., 2005; Peter et al., 2006; Jensen and Pfister, 2005; Gao et al., 2004).

In general ice nucleation in aqueous inorganic systems which have been tested to low temperature (< 200 K) are consistent with the water activity criterion (Koop, 2004; Murray and Bertram, 2008). However, very few studies exist in which homogeneous freezing has been measured in aqueous organic solution droplets (Prenni et al., 2001; Wise et al., 2004; Zobrist et al., 2006) and non have been performed for conditions relevant for the TTL (i.e. < 200 K).

Organic material accounts for up to 70% of the mass of fine aerosol in the troposphere (McFiggans et al., 2005). Much of this organic material is oxygenated and COOH, OH and C=O functional groups are ubiquitous (Graber and Rudich, 2006; Saxena and Hildemann, 1996). In-situ single particle mass spectrometry measurements

Inhibition of ice crystallisation

B. J. Murray

Title Page

Abstract

Introduction

Conclusions

References

Tables

Figures

◀

▶

◀

▶

Back

Close

Full Screen / Esc

Printer-friendly Version

Interactive Discussion



of UT aerosol confirm that oxygenated organic material is usually present, and in some cases organic material is the dominant component of aerosol (Cziczo et al., 2004a, b; Murphy et al., 2006, 1998; Zobrist et al., 2006). An important property of oxygenated organic compounds is that they can form extensive hydrogen bonding and molecules of relatively large mass may therefore be soluble in water.

There is mounting evidence that organic rich aerosol behave differently to sulphate aerosol. Cziczo et al. (2004a) found organic-rich particles preferentially remain unfrozen in the atmosphere, which suggested organic aerosol may behave differently to inorganic aerosol. Using a thermal diffusion chamber at 229K and a single particle mass spectrometer, DeMott et al. (2003) demonstrated that aerosols composed of organics froze at a significantly higher saturation threshold than sulphate aerosol. In a set of expansion chamber experiments Möhler et al. (2005) found that soot composed of 40% organic carbon nucleated ice inefficiently even at an RH_{lh} (relative humidity with respect to hexagonal ice) 190%; this is well above the nucleation threshold defined by the water activity criterion ($RH_{lh} \sim 160\%$).

In the present experimental study the crystallisation of aqueous citric acid (2-hydroxypropane-1,2,3-tricarboxylic acid, $C_6H_8O_7$) solution droplets have been investigated using X-ray diffraction. Citric acid was chosen for this study for two main reasons. First, it contains one hydroxyl (OH) and three carboxylic (COOH) functional groups and therefore has similar functionality to many compounds in atmospheric aerosol. Indeed, it has been observed as a minor component of atmospheric aerosol (Saxena and Hildemann, 1996; Falkovich et al., 2005). The second reason for choosing citric acid for these experiments is that the physical properties of aqueous citric acid solutions have been characterised since it is a common ingredient in food and pharmaceutical products. The properties include the glass transition temperature (Maltini et al., 1997). This is the temperature below which the viscosity of a liquid becomes so great that it transforms into an amorphous (non-crystalline; i.e. no long range order) solid. These amorphous solids are often referred to as glassy solids and neither nucleation nor crystallisation is expected.

Inhibition of ice crystallisation

B. J. Murray

Title Page

Abstract

Introduction

Conclusions

References

Tables

Figures

◀

▶

◀

▶

Back

Close

Full Screen / Esc

Printer-friendly Version

Interactive Discussion



**Inhibition of ice
crystallisation**

B. J. Murray

Title Page

Abstract

Introduction

Conclusions

References

Tables

Figures

◀

▶

◀

▶

Back

Close

Full Screen / Esc

Printer-friendly Version

Interactive Discussion



The objective of this laboratory investigation was to investigate the impact of an oxygenated organic compound relevant for the Earth's atmosphere on the nucleation and growth of ice crystals in aqueous droplets. In order to do this, droplets of known composition were frozen within an X-ray diffractometer. The resulting diffraction patterns of the droplets were used to determine the phase change temperatures and also the quantity of ice that crystallised. It is found that the crystallisation of ice is incomplete below ~ 197 K. It is shown that this inhibition of crystallisation is most likely related to the high viscosity of citric acid solutions at temperatures relevant for the TTL. Finally, the implications of highly viscous or glassy solution droplets for UT cloud formation are discussed.

2 Experimental

A powder X-ray diffractometer equipped with a cold stage has been employed to investigate the crystallisation of aqueous citric acid solution droplets. This PANalytical X'Pert instrument, in Bragg-Brentano reflection geometry, was equipped with a Cu K_{α} X-ray source and X'Celerator detector.

Aqueous solutions were prepared gravimetrically with a balance accurate to 2×10^{-3} g (0 to 61.2 wt%) and then mixed with an oil phase, which consisted of 10 wt% lanoline surfactant in paraffin mineral oil. The oil and surfactant were insoluble in the aqueous phase. The proportion of aqueous phase in oil phase was also recorded gravimetrically. A few millilitres of emulsion were prepared using a magnetic stirrer; this produced droplets of volume median diameter between 5–10 μm .

There are a number of reasons for employing emulsified samples in these experiments. First, if nucleation should occur heterogeneously, crystallisation will be contained within individual droplets since they are separated by oil; hence, homogeneous nucleation is the dominant mode. Second, each droplet crystallises independently of the next, hence there is no preferred crystallographic orientation in the sample overall. Preferred orientation can significantly alter the relative intensities of the diffraction

patterns and is observed in samples of ice deposited on a surface from the gas phase (Dowell and Rinfret, 1960; Shilling et al., 2006). The diffraction patterns here and in previous X-ray diffraction experiments employing emulsions exhibit no signs of preferred orientation (Murray and Bertram, 2006, 2007a, b; Murray et al., 2005). Third, the solute concentration of the solution droplets is fixed, which simplifies the interpretation of the data.

There are suggestions in the literature that nucleation occurs at the surface of droplets (Tabazadeh et al., 2002). If this were the case one might expect the surfactant to influence nucleation. However, there are no significant differences in freezing temperatures of droplets in emulsions and those on a hydrophobic surface; this suggests the surfactant and oil phase do not interfere with the nucleation process in micrometer sized droplets (Bertram et al., 2000). In addition measurements of nucleation in micrometer sized droplets are consistent with nucleation in the volume rather than at the surface (Duft and Leisner, 2004).

About 0.1 ml of the emulsion was placed in the sample holder on the cold stage (Anton-Paar TTK 450) which was initially held at room temperature. The temperature of the droplets was then ramped down at an average rate of $5 \pm 1 \text{ K min}^{-1}$ to 173 K. As the droplets were cooled the ramp was paused for $\sim 30 \text{ s}$ every 5 or 10 K, in order to measure the diffraction pattern around the ice peak at $2\theta = 40^\circ$. Hence, the temperatures over which ice formed in the droplets could be determined by the growth of this peak out of the amorphous background; this is referred to as the freezing temperature. Once at low temperature (173 K) the full diffraction pattern was measured between $2\theta = 20$ and 50° , which covers all major peaks in both cubic and hexagonal ice. Phase changes on warming were measured in much the same way as was done for freezing. An average ramp of $5 \pm 1 \text{ K min}^{-1}$, with intervals of 5 K were used when monitoring ice growth on warming, referred to as warm ice crystallisation, and an average ramp of $1 \pm 0.1 \text{ K min}^{-1}$ and 1 K intervals were used to determine ice melting temperatures.

Inhibition of ice crystallisation

B. J. Murray

Title Page

Abstract

Introduction

Conclusions

References

Tables

Figures

◀

▶

◀

▶

Back

Close

Full Screen / Esc

Printer-friendly Version

Interactive Discussion



3 Results and discussion

3.1 Diffraction patterns of frozen droplets

Example of typical diffraction patterns of citric acid solution droplets which had been cooled to 173 K at 5 K min^{-1} are shown in Fig. 1. There are clearly some very strong differences between these patterns. Pattern 1a is of frozen 20.6 wt% solution droplets which froze at $224 \pm 6 \text{ K}$. This pattern is consistent with previous diffraction patterns of a mixture of cubic ice (ice I_c) and hexagonal ice (ice I_h) (Murray and Bertram, 2006; Murray and Bertram, 2007a, b; Murray et al., 2005). Pattern 1b is that of 32.4 wt% solution droplets which froze at $219 \pm 6 \text{ K}$. In this pattern several of the peaks unique to hexagonal ice are absent and the pattern is consistent with ice I_c with stacking faults (Murray et al., 2005). A strong solute dependence of the ice phase has been observed in the past, with $(\text{NH}_4)_3\text{H}(\text{SO}_4)_2$ freezing to ice I_c below 200 K, whereas a similar amount of ice I_c will only form below 183 K in NH_4HSO_4 solution droplets (Murray and Bertram, 2007b; Murray and Bertram, 2008). It seems that citric acid solution droplets have an even greater propensity to freeze to the metastable ice I_c than $(\text{NH}_4)_3\text{H}(\text{SO}_4)_2$ droplets, with a threshold $\sim 20 \text{ K}$ higher. The issue of ice phase in organic solution droplets has been addressed in a separate manuscript (Murray, 2008).

The pattern shown in Fig. 1c is that of droplets of 58.2 wt% citric acid which were cooled to 173 K at the standard rate of 5 K min^{-1} . The major ice peaks at $2\theta = 40$ and 47° (common to both ice I_c and ice I_h) are absent, indicating that no bulk ice crystallised. There is a hint of an ice peak at $2\theta = 24^\circ$, which indicates that there is limited crystalline nature and that ice nucleation may have begun, but it did not continue. The inhibition of crystallisation will be discussed at length later in this paper.

3.2 Phase changes in the citric acid-water system

The temperatures at which freezing (T_f), ice crystallisation on warming (T_w) and ice melting (T_m) occurred are plotted in Fig. 2 (these terms are defined in Sect. 2). This

Inhibition of ice crystallisation

B. J. Murray

Title Page

Abstract

Introduction

Conclusions

References

Tables

Figures

◀

▶

◀

▶

Back

Close

Full Screen / Esc

Printer-friendly Version

Interactive Discussion



**Inhibition of ice
crystallisation**

B. J. Murray

Title Page

Abstract

Introduction

Conclusions

References

Tables

Figures

◀

▶

◀

▶

Back

Close

Full Screen / Esc

Printer-friendly Version

Interactive Discussion



diagram is referred to as a state diagram, rather than a phase diagram, since both equilibrium and kinetically controlled phase changes are shown. Previous measurements of T_m of citric acid solutions are also plotted and are in agreement with those from the present study. In addition the melting and freezing temperatures of pure water are consistent with literature values.

Freezing temperatures have been recorded for droplets with concentrations up to 49.2 wt%. Insufficient ice crystallised in droplets of higher concentration to identify a freezing temperature (the technique for measuring crystallisation temperatures with XRD is sensitive to ~ 10 wt% of the overall mass of the droplets changing phase). Ice crystallisation was not observed in droplets of < 49.2 wt% on cooling, but in some cases ice crystal growth was detected at 211 ± 6 K as the droplets were warmed at 5 K min^{-1} . Ice crystallised on warming droplets with concentrations of up to 58.2 wt% and melting temperatures were determined. However, T_w was determined for droplets of concentration > 54.4 wt%. The fact that ice crystallised on warming indicates that nucleation of ice took place at some lower temperature, but crystal growth rates only became comparable to the warming rate at around 211 K. Droplets with concentrations of 59.6 and 61.2 wt% did not crystallise on cooling to 173 K or on subsequent warming indicating that nucleation of ice did not occur at all in these very concentrated solution droplets.

It has been shown in the past that the homogeneous freezing temperature depression of an aqueous solution $\{\Delta T_f = T_f(\text{Pure H}_2\text{O}) - T_f(\text{solution})\}$ increases in direct proportion to the melting point depression $\{\Delta T_m = T_m(\text{Pure H}_2\text{O}) - T_m(\text{solution})\}$. This is true for a wide range of inorganic (DeMott, 2002) and organic solutions (Zobrist et al., 2003). Figure 3 shows that citric acid solution droplets behave in a similar manner, with a slope, λ ($\Delta T_f / \Delta T_m$), of 2.24 ± 0.06 . Literature values for smaller solute molecules (e.g. H_2SO_4 , NaCl, KCl, etc.) have λ values of between 1.4–2.2, while larger more complex molecules capable of extensive hydrogen bonding have λ values up to 5.1 (Zobrist et al., 2003). Zobrist and Koop (Zobrist et al., 2003) suggest that the more extensive hydrogen bonding between oxygenated organic molecules and water, compared to many inorganic solutes, leads to larger values of λ .

Inhibition of ice crystallisation

B. J. Murray

Title Page

Abstract

Introduction

Conclusions

References

Tables

Figures

◀

▶

◀

▶

Back

Close

Full Screen / Esc

Printer-friendly Version

Interactive Discussion



If we assume that the delay between nucleation and crystallisation is negligible for the points shown in Fig. 3, we can say that the measured ΔT_f is the same as the nucleation point depression (ΔT_n). Hence, the relationship $\Delta T_n = \lambda \Delta T_m$ ($\lambda = .24 \pm 0.06$) can be used to estimate T_n in the cases where freezing was not observed, but where ice crystallised on warming and T_m was measured. In Fig. 2, values of T_n based on this relationship have been plotted for citric acid concentrations from 0 to 58.2 wt%, where T_m was measured experimentally.

3.3 Inhibition of ice crystallisation

In Fig. 4, the fraction of water which crystallised to ice $\{X_{ice} = M_{ice} / (M_{ice} + M_{liq})\}$, where M_{ice} is the mass of ice and M_{liq} is the mass of water in the aqueous phase} is plotted as a function of ice nucleation temperature (T_n). X_{ice} was determined by measuring the area under the ice peak at $2\theta = 40^\circ$ in the full diffraction patterns recorded at 173 K (such as those in Fig. 1). Peak areas were determined by fitting a Gaussian profile to the pertinent peak using a least-squared routine and integrating the area under the fitted profile. This technique was used in the past to deconvolute overlapping peaks (Murray and Bertram, 2007b). The area of this peak, I_{40} , was then normalized to the weight fraction of water in the solution droplets, W_{H_2O} , and the weight fraction of solution in oil phase, W_{sol} , i.e. the normalized peak area, $L_{40} = I_{40} / W_{H_2O} / W_{sol}$. The normalized peak area of the frozen solution droplets was then divided by the value for frozen pure water droplet in order to obtain the fraction of water crystallised, i.e. $X_{ice} = L_{40}(\text{solution}) / L_{40}(\text{pure } H_2O)$ and since diffraction intensity is proportional to mass $X_{ice} = M_{ice} / (M_{ice} + M_{liq})$. It is assumed here that 100% of water in pure water droplets crystallises to ice. Hence, a value of 1 indicates 100% of the water crystallised and 0 indicates 0% of the water crystallised.

The maximum fraction of water that can crystallise ($X_{ice}(\text{max})$) in aqueous citric acid solution droplets assuming there are no kinetic limitations to ice crystal growth and that the solute phase does not crystallise is shown in Fig. 4. When ice crystallises in a solution droplet it will exist in equilibrium with aqueous brine if there are no kinetic

limitations to crystal growth. Hence some fraction of water will necessarily be in the aqueous phase and $X_{\text{ice}}(\text{max})$ will therefore be less than unity when ice forms in a solution. In the experiments presented here, citric acid was not observed to crystallise, hence when ice formed it was always internally mixed with aqueous citric acid brine.

If ice was in equilibrium with aqueous citric acid when the full diffraction patterns were measured at 173 K, then the concentration of this brine would dictate $X_{\text{ice}}(\text{max})$ for a particular initial solution concentration. The determination of the ice-liquid line in Fig. 3 is described in Appendix A, and it was found that the concentration of an aqueous citric acid brine in equilibrium with ice at 173 K was 83.0 wt%. The increase in aqueous phase concentration from the initial solution before ice formation to the final concentration after ice formation is due to water being removed from the aqueous phase to form ice; hence the $X_{\text{ice}}(\text{max})$ was quantified.

Inspection of Fig. 4 reveals that the experimentally determined values of X_{ice} are significantly smaller than $X_{\text{ice}}(\text{max})$, in all cases except for very dilute solution or pure water. This indicates that there is some kinetic limitation to ice crystal growth. In fact, X_{ice} drops dramatically below 197 ± 6 K indicating that crystallisation of ice is strongly inhibited below this temperature when cooled at 5 K min^{-1} . No detectable bulk ice crystallised in these droplets (i.e. less than 3% of the available water crystallised; as determined from the full diffraction patterns which were collected over 30–40 min at 173 K). This is an important finding since it is generally assumed that ice will nucleate and grow in aqueous droplets under conditions relevant for the Earth's troposphere. In fact, ice crystallised readily in NH_4HSO_4 solution droplets at temperatures well below 198 K (open green triangles in Fig. 4); in agreement with previous experiments (Koop et al., 1999; Murray and Bertram, 2008). The freezing of citric acid solution droplets clearly contrasts with that of NH_4HSO_4 droplets and may have important implications for ice cloud formation in the TTL region. These implications are discussed later in this paper.

Inhibition of ice crystallisation

B. J. Murray

Title Page

Abstract

Introduction

Conclusions

References

Tables

Figures

◀

▶

◀

▶

Back

Close

Full Screen / Esc

Printer-friendly Version

Interactive Discussion



3.4 The formation of highly viscous or glassy solution droplets

The experiments presented here show that ice crystallisation is inhibited in citric acid solution droplets below 197 ± 6 K. It is suggested here that these solution droplets become highly viscous or even glassy and crystallisation is therefore inhibited. Unfortunately, no direct measurements exist of diffusion in low temperature citric acid solution droplets. However, the glass transition temperature (T_g) for several pertinent concentrations of citric acid solution have been measured and fitted (Maltini et al., 1997); these are plotted in Fig. 5. The T_g provides a useful reference temperature from which we can estimate viscosity and diffusion at higher temperatures. The measured and fitted T_g 's have been used to estimate the root mean square distance water molecules diffuse in 60 s ($x_{\text{H}_2\text{O}}$) and lines of constant $x_{\text{H}_2\text{O}}$ are plotted in Fig. 5. The derivation of $x_{\text{H}_2\text{O}}$ is described in Appendix B.

The lines of constant $x_{\text{H}_2\text{O}}$ in Fig. 5 (values are in micrometers) provide a useful means with which to gauge if a droplet is likely to crystallize. The exact relationship between diffusion and crystal growth is complicated. However, it is true that if $x_{\text{H}_2\text{O}}$ is much smaller than the dimensions of the droplets then ice will not readily crystallise.

Inspection of Fig. 5 shows that in general that molecular diffusion decreases dramatically as concentration increases and temperature decreases. It is clear from Fig. 4 the crystallisation did not occur below 197 ± 6 K in droplets which were cooled to 173 K at a rate of 5 K min^{-1} . This corresponds to a diffusion distance of $0.09\ \mu\text{m}$ in Fig. 5 and defines $x_{\text{H}_2\text{O}}$ below which crystallisation at a cooling rate of 5 K min^{-1} is limited by diffusion. Crystallisation only occurs on warming these solution droplets at 5 K min^{-1} when $x_{\text{H}_2\text{O}} > 0.09\ \mu\text{m}$. The $x_{\text{H}_2\text{O}}$ contour for $x_{\text{H}_2\text{O}} = 0.09\ \mu\text{m}$ is plotted as a green line in Fig. 5 and represents the limiting condition for crystal growth for a warming or cooling rate of 5 K min^{-1} . At temperatures above this line, crystal growth is rapid on the minute timescale, whereas at lower temperatures ice crystal growth is slow.

Droplets were cooled at a rate of 5 K min^{-1} in these experiments, which is significantly faster than typical cooling rates leading to cirrus cloud formation (0.0007 to

Inhibition of ice crystallisation

B. J. Murray

Title Page

Abstract

Introduction

Conclusions

References

Tables

Figures

◀

▶

◀

▶

Back

Close

Full Screen / Esc

Printer-friendly Version

Interactive Discussion



**Inhibition of ice
crystallisation**

B. J. Murray

Title Page

Abstract

Introduction

Conclusions

References

Tables

Figures

◀

▶

◀

▶

Back

Close

Full Screen / Esc

Printer-friendly Version

Interactive Discussion



0.7 K min⁻¹, Jensen et al., 2005). The threshold of 197 K, below which ice crystallisation becomes inhibited at a cooling rate of 5 K min⁻¹, will shift to lower temperatures for slower cooling rates. If an air parcel is cooling at 0.5 K min⁻¹, then the time available for crystal growth will be a factor of ten longer than in the experiments with cooling at 5 K min⁻¹. Hence, we can then say that crystallisation will only become inhibited when $x_{\text{H}_2\text{O}} > 0.009 \mu\text{m}$ (the orange line in Fig. 5) and that this corresponds to a T_n of 192 K.

In droplets of 59.6 and 61.2 wt% no crystallisation was observed on cooling to 173 K, leaving them at 173 K for ~40 min or on warming them at 5 K min⁻¹. It appears that the nucleation of ice itself was inhibited. Inspection of the predicted nucleation temperature of ice in citric acid droplets in Fig. 5 reveals that the nucleation temperature intercepts T_g at around 58.5 wt% and 180 K. This is consistent with the measurement that nucleation does not take place in 59.6 and 61.2 wt% solution droplets; in fact, these droplets most likely formed glassy solids. Hence the point where the homogeneous freezing temperature and glass transition temperature intercept represents a limit of nucleation.

In an investigation of freezing in aqueous H₂SO₄ solution droplets, Koop et al. (1998) found that droplets of concentration greater than 26.7 wt% did not crystallise on cooling, but did on warming at 10 K min⁻¹ between 165 and 172 K. Bogdan et al. (2006) made a similar observation in 31.5 wt% H₂SO₄ solution droplets, although the crystallisation on warming at 3 K min⁻¹ took place at ~156 K. This behaviour is similar to citric acid solutions, except that crystallisation occurred at much lower temperatures in aqueous H₂SO₄. This indicates that diffusion becomes rapid, in comparison to ramp rate, at much lower temperatures in H₂SO₄ solutions than in citric acid solutions. In fact, the glass transition measured by Bogdan (for 31.5 wt% H₂SO₄ droplets) was at ~142 K; this is about 14 K below the temperature at which the droplets crystallised when warming at 3 K min⁻¹. Given crystallisation becomes rapid in H₂SO₄ solutions at temperatures well below those typical for the Earth's troposphere, ice would be expected to form in these aerosols efficiently and in accord with the water activity criterion (Koop et al., 2000). Whereas, in citric acid solution droplets ice formation may occur at a slower rate or may even be inhibited.

It is well known that T_g of aqueous solutions depends strongly on the solute type. In fact, Zobrist et al. (2008) have very recently demonstrated that T_g for a number of aqueous inorganic solutions are much lower than for a number of atmospherically relevant organic acid and polyol solutions. They conclude that aqueous organic droplets may form glasses in the atmosphere. This is consistent with the results of the present study.

4 Atmospheric implications and summary

The primary conclusion from this experimental study is that ice does not necessarily crystallise in aqueous solution droplets even if they are sufficiently supersaturated for homogeneous nucleation. The growth of ice crystals in citric acid droplets is much slower below 197 ± 6 K than in ammonium bisulphate (or sulphuric acid) solution droplets and did not occur when cooled at 5 K min^{-1} . It is argued that crystallisation is limited by slow diffusion in these highly viscous solution droplets. It is predicted that ice crystal growth is limited below ~ 192 K at an atmospherically relevant cooling rate of 0.5 K min^{-1} . Nucleation does not occur in solution droplets where sufficient supersaturation for nucleation is only attained below the glass transition temperature; in the case of aqueous citric acid this threshold is at ~ 180 K. This work extends that of Koop et al. (2000) who showed that the temperature at which ice nucleates homogeneously is a function of water activity only. Here, it is argued that solution viscosity plays a critical role in i, the growth of ice crystals within solution droplets and ii, the nucleation of ice.

The inhibition of ice crystallisation may have important implications for cloud formation in the tropical tropopause layer where temperatures are regularly as low as ~ 186 K (Zhou et al., 2004). If the crystallisation of ice is inhibited within atmospheric aqueous solution droplets in an ascending air mass, then the humidity will exceed the limit defined by the water activity criterion (Koop et al., 2000). In fact, field measurements appear to show extreme supersaturations, with RH_{lh} in excess of 200% with no apparent ice cloud formation (Jensen et al., 2005). These very high supersatu-

Inhibition of ice crystallisation

B. J. Murray

Title Page

Abstract

Introduction

Conclusions

References

Tables

Figures

◀

▶

◀

▶

Back

Close

Full Screen / Esc

Printer-friendly Version

Interactive Discussion



Inhibition of ice crystallisation

B. J. Murray

Title Page

Abstract

Introduction

Conclusions

References

Tables

Figures

◀

▶

◀

▶

Back

Close

Full Screen / Esc

Printer-friendly Version

Interactive Discussion



rations were observed in air that was below 190 K. This is in the temperature range where organic acids, similar to citric acid, might inhibit ice crystallisation, but where sulphate aerosols would be expected to freeze readily and lead to cloud formation. It is suggested here that very high supersaturations might result in any very cold air mass where the aerosol contains sufficient oxygenated organic material to inhibit ice crystallisation. Unfortunately no composition data was obtained on the aerosol in this layer of very high supersaturation observed by Jensen et al. (2005). However, particles sampled nearby were composed of typical sulphate-organic mixtures (Jensen et al., 2005).

Atmospheric aerosols contain a massive range of organic species (Saxena and Hildemann, 1996) usually internally mixed with sulphate (Murphy et al., 2006), hence real aqueous droplets will have a range of viscosities. The ubiquity of carboxylic, hydroxyl, carbonyl and other functional groups, which are capable of hydrogen bonding, in the organic fraction of aerosol suggests that many oxygenated organic solutes will have a similar impact on freezing to citric acid. It is possible some will slow crystal growth even more dramatically than citric acid, while others will behave more like sulphate aerosol. Further experiments are required to test crystallisation in other aqueous oxygenated organic solutions and also in aqueous organic-sulphate mixtures.

This study represents a first step in understanding the role of viscosity on cold ice cloud formation. While it is clearly shown that ice crystallisation can be inhibited in citric acid solution droplets it should be noted that the trajectory through the temperature-composition phase diagram is very different in the experiments presented here and for droplets in the atmosphere. In the experiments presented here, solution concentration is fixed by locking droplets in an oil emulsion and droplets are then cooled. Whereas, aerosols in an atmospheric air parcel will take up water to become more dilute as they cool down, only freezing when they become sufficiently dilute and cold. However, in the case of citric acid solution droplets this will involve starting with highly concentrated solution droplets on the right hand side of Fig. 5 which may already be highly viscous or glassy. If droplets start off in a highly viscous or glassy state then it is unlikely that they

will take up water and dilute. Hence, the droplets may not become sufficiently dilute for ice to nucleate homogeneously within them.

On account of both the inhibition of ice crystallisation and the likely limited uptake of water into highly viscous organic acid solution droplets it seem probable that ice crystallisation should be preferred in atmospheric droplets rich in sulphate. In fact, in a single particle mass spectrometry study of cirrus ice crystals and aerosol (mentioned in the introduction) Cziczo et al. (2004a) found that sulphate preferentially partitioned to the ice phase over organic material. In a modelling study, Kärcher and Koop (2005) suggested a slower uptake of water by organic containing droplets might explain this observation. They argued that a coating of organic material at the air-water interface may reduce the condensation coefficient of water. An alternative explanation for the observation is that organic containing droplets are highly viscous at sufficiently low temperature and therefore i, do not take up water as efficiently as aqueous sulphate droplets and ii, even if ice does nucleate, crystal growth rates are slower than in sulphate droplets.

In order to fully asses the impact of ultra-viscous liquids on cloud formation, further research is needed. This should include measurements of ice crystallisation in solution droplets with solutes other than citric acid, water uptake into viscous droplets and cloud chamber simulations in order follow a more atmospherically relevant temperature-RH trajectory. Nevertheless, in this paper it has been shown that droplets which contain a solute of similar functionality to many molecules ubiquitous to the troposphere appear to become highly viscous under TTL conditions and crystallisation of ice can be inhibited.

Inhibition of ice crystallisation

B. J. Murray

Title Page

Abstract

Introduction

Conclusions

References

Tables

Figures

◀

▶

◀

▶

Back

Close

Full Screen / Esc

Printer-friendly Version

Interactive Discussion



Determination of the hexagonal ice-liquid equilibrium curve

The ice-liquid curve has been described in terms of solution water activity (a_w) between 150 and 273 K and is independent of solute type (see Eqs. (1) and (2) in Koop et al., 2000). In order to plot the ice-liquid equilibrium curve as a function of citric acid solution concentration (as it is in Fig. 5) the relationship between a_w and solution concentration must be known. Values of a_w as a function of citric acid concentration are plotted in Fig. A1 and a list of data sources is given in Table A1. Some of the sources of data quote values of a_w which are plotted in Fig. A1 unaltered (Levien, 1955; Maffia and Meirelles, 2001; Peng et al., 2001). Apelblat et al. (1995) quote the difference in vapour pressure between pure water and an aqueous citric acid solution. This data could be used to derive a_w using the known vapour pressure of pure water (Murphy and Koop, 2005). As mentioned above there is a direct relationship between a_w and ice melting temperatures. Hence, melting temperatures can be used as a measure of a_w . Using Eqs. (1) and (2) from Koop et al. (2000) water activity was determined from ice melting temperatures from the literature (Apelblat, 2003; Taylor, 1926) and from the current experiments.

The data in Fig. A1 have been parameterised using a polynomial equation of the form

$$a_w = A + Bc + Cc^2 + Dc^3 + Ec^4 + Fc^5 \quad (\text{A1})$$

Where c is the concentration in wt% and $A=1$, $B=-2.3900 \times 10^{-3}$, $C=1.5000 \times 10^{-4}$, $D=-6.1599 \times 10^{-6}$, $E=8.7490 \times 10^{-8}$ and $F=-5.1132 \times 10^{-10}$.

In order to determine the dependence of the ice-liquid equilibrium temperature on concentration, it is assumed that a_w is independent of temperature. Water activity for aqueous citric acid solutions are plotted for temperatures ranging from 250.7 to 319.33 K in Fig. A1. There is not a strong dependence of a_w in this temperature range; if there were the results would be scattered around the line of best fit. A significant

Inhibition of ice crystallisation

B. J. Murray

Title Page

Abstract

Introduction

Conclusions

References

Tables

Figures

◀

▶

◀

▶

Back

Close

Full Screen / Esc

Printer-friendly Version

Interactive Discussion



Inhibition of ice crystallisation

B. J. Murray

Title Page

Abstract

Introduction

Conclusions

References

Tables

Figures

◀

▶

◀

▶

Back

Close

Full Screen / Esc

Printer-friendly Version

Interactive Discussion



dependence of a_w at lower temperatures can not be ruled out; however, similar assumptions have been made and justified in the past in other aqueous systems (Koop et al., 2000). The ice-liquid equilibrium curve in Fig. 5 was therefore calculated using Eq. (A1) and Eqs. (1) and (2) from Koop et al. (2000).

5 Appendix B

Determination of the lines of constant $x_{\text{H}_2\text{O}}$ in Fig. 5

No measurements of molecular diffusion exist in low temperature citric acid solutions. However, the glass transition temperature in aqueous citric acid is known and a method of estimating molecular diffusion based on the T_g is outline here. It is well know that viscosity above T_g in aqueous solutions increases extremely rapidly with decreasing temperature (Angel, 2002) and can be described by the WLF (Williams-Landel-Ferry) equation (Debenedetti, 1996):

$$\log \eta_T = \log \eta_{T_g} - \left(\frac{17.44(T - T_g)}{51.6 + (T - T_g)} \right) \quad (\text{B1})$$

15 where η_T is the viscosity at temperature T , η_{T_g} is the viscosity at T_g and the numerical values are given by Debenedetti (1996). The relationship between molecular diffusion (D) of species i and viscosity can be approximated by the Stokes-Einstein equation (Debenedetti, 1996):

$$D_i = \frac{kT}{6\pi\eta_T r_i} \quad (\text{B2})$$

20 Where k is the Boltzmann constant and r_i is the hydrodynamic radius of i . This relationship should be considered an approximation, since the relationship between diffusion and viscosity becomes complex in aqueous solutions at temperatures close to the glass transition (Debenedetti, 1996).

The root mean square distance molecules of species i diffuse in a time (t) can be expressed as

$$x_i = (6D_i t)^{0.5} \quad (\text{B3})$$

Lines of constant mean diffusion distance for water molecules ($x_{\text{H}_2\text{O}}$) are plotted in Fig. 5 for a time period of 60 s. In order to determine $x_{\text{H}_2\text{O}}$, $r_{\text{H}_2\text{O}}$ was assumed to be the same in citric acid solutions as it is in supercooled water at 244 K (i.e. $r_{\text{H}_2\text{O}}=0.94 \text{ \AA}$, given that $D_{\text{H}_2\text{O}}=1.9 \times 10^{-10} \text{ m}^2 \text{ s}^{-1}$ and $\eta=10 \text{ cP}$ in supercooled water at 244 K (Debenedetti, 1996)) and η_{Tg} was taken as 10^{14} cP .

Acknowledgements. The author thanks D. Wright for help running the X-ray diffractometer and A. K. Bertram, T. Koop, S. Dobbie, O. Möhler and T. Leisner for helpful discussions. The author acknowledges the Natural Environment Research Council and the School of Chemistry for funding (NE/D009308/1).

References

- Abbatt, J. P. D.: Interactions of atmospheric trace gases with ice surfaces: Adsorption and reaction, *Chem. Rev.*, 103, 4783–4800, 2003.
- Angel, C. A.: Liquid fragility and the glass transition in water and aqueous solutions, *Chem. Rev.*, 102, 2627–2650, 2002.
- Apelblat, A., Dov, M., Wisniak, J., and Zabicky, J.: Osmotic and activity coefficients of HO₂CCH₂C(OH)(CO₂H)CH₂CO₂H (citric acid) in concentrated aqueous solutions at temperatures from 298.15 k to 318.15 k, *J. Chem. Thermodyn.*, 27, 347–353, 1995.
- Apelblat, A.: Cryoscopic studies in the citric acid-water system, *J. Mol. Liq.*, 103-104, 201–210, 2003.
- Bertram, A. K., Koop, T., Molina, L. T., and Molina, M. J.: Ice formation in (NH₄)₂SO₄-H₂O particles, *J. Phys. Chem. A*, 104, 584–588, 2000.
- Bogdan, A., Molina, M. J., Sassen, K., and Kulmala, M.: Formation of low-temperature cirrus from h₂so₄/h₂o aerosol droplets, *J. Phys. Chem. A*, 110, 12541–12542, 2006.

Inhibition of ice crystallisation

B. J. Murray

Title Page

Abstract

Introduction

Conclusions

References

Tables

Figures

◀

▶

◀

▶

Back

Close

Full Screen / Esc

Printer-friendly Version

Interactive Discussion



**Inhibition of ice
crystallisation**

B. J. Murray

Title Page

Abstract

Introduction

Conclusions

References

Tables

Figures

◀

▶

◀

▶

Back

Close

Full Screen / Esc

Printer-friendly Version

Interactive Discussion



- Cziczo, D. J., DeMott, P. J., Brooks, S. D., Prenni, A. J., Thomson, D. S., Baumgardner, D., Wilson, J. C., Kreidenweis, S. M., and Murphy, D. M.: Observations of organic species and atmospheric ice formation, *Geophys. Res. Lett.*, 31, L12116, doi:10.1029/2004GL019822, 2004a.
- 5 Cziczo, D. J., Murphy, D. M., Hudson, P. K., and Thomson, D. S.: Single particle measurements of the chemical composition of cirrus ice residue during crystal-face, *J. Geophys. Res.-Atmos.*, 109, D04201, doi:10.1029/2003JD004032, 2004b.
- Debenedetti, P. G.: *Metastable liquids concepts and principles*, Princeton University Press, New Jersey, 1996.
- 10 DeMott, P. J.: Laboratory studies of cirrus cloud processes, in: *Cirrus*, edited by: Lynch, D. K., Sassen, K., Starr, D. C., and Stephens, G., Oxford University Press, Oxford, 102–135, 2002.
- DeMott, P. J., Cziczo, D. J., Prenni, A. J., Murphy, D. M., Kreidenweis, S. M., Thomson, D. S., Borys, R., and Rogers, D. C.: Measurements of the concentration and composition of nuclei for cirrus formation, *Proc. Natl. Acad. Sci. USA*, 100, 14 655–14 660, 2003.
- 15 Denman, K. L., Brasseur, G., Chidthaisong, A., Ciais, P., Cox, P. M., Dickinson, R. E., Hauglustaine, D., Heinze, C., Holland, E., Jacob, D., Lohmann, U., Ramachandran, S., da Silva Dias, P. L., Wofsy, S. C., and Zhang, X.: Couplings between changes in the climate system and biogeochemistry, in: *Climate change 2007: The physical science basis*, Contribution of working group I to the fourth assessment report of the intergovernmental panel on climate change, edited by: Solomon, S. D., Qin, M., Manning, Z., Chen, M., Marquis, K. B., Averyt, M. T., and Miller, H. L., Cambridge University Press, Cambridge, 2007.
- 20 Dowell, L. G. and Rinfret, A. P.: Low-temperature forms of ice as studied by x-ray diffraction, *Nature*, 188, 1144–1148, 1960.
- Duft, D. and Leisner, T.: Laboratory evidence for volume-dominated nucleation of ice in supercooled water microdroplets, *Atmos. Chem. Phys.*, 4, 1997–2000, 2004, <http://www.atmos-chem-phys.net/4/1997/2004/>.
- Falkovich, A. H., Graber, E. R., Schkolnik, G., Rudich, Y., Maenhaut, W., and Artaxo, P.: Low molecular weight organic acids in aerosol particles from rondonia, brazil, during the biomass-burning, transition and wet periods, *Atm. Chem. Phys.*, 5, 781–797, 2005.
- 30 Gao, R. S., Popp, P. J., Fahey, D. W., Marcy, T. P., Herman, R. L., Weinstock, E. M., Baumgardner, D. G., Garrett, T. J., Rosenlof, K. H., Thompson, T. L., Bui, P. T., Ridley, B. A., Wofsy, S. C., Toon, O. B., Tolbert, M. A., Karcher, B., Peter, T., Hudson, P. K., Weinheimer, A. J., and Heymsfield, A. J.: Evidence that nitric acid increases relative humidity in low-temperature

**Inhibition of ice
crystallisation**

B. J. Murray

Title Page

Abstract

Introduction

Conclusions

References

Tables

Figures

◀

▶

◀

▶

Back

Close

Full Screen / Esc

Printer-friendly Version

Interactive Discussion



cirrus clouds, *Science*, 303, 516–520, 2004.

Gettelman, A. and Forster, P. M. D.: A climatology of the tropical tropopause layer, *J. Meteorol. Soc. Jpn*, 80, 911–924, 2002.

Graber, E. R. and Rudich, Y.: Atmospheric humilis: How humic-like are they? A comprehensive and critical review, *Atmos. Chem. Phys.*, 6, 729–753, 2006,
<http://www.atmos-chem-phys.net/6/729/2006/>.

Jensen, E. and Pfister, L.: Implications of persistent ice supersaturation in cold cirrus for stratospheric water vapor, *Geophys. Res. Lett.*, 32, D03208, doi:10.101029/2004GL021125, 2005.

Jensen, E. J., Smith, J. B., Pfister, L., Pittman, J. V., Weinstock, E. M., Sayres, D. S., Herman, R. L., Troy, R. F., Rosenlof, K., Thompson, T. L., Fridlind, A. M., Hudson, P. K., Cziczo, D. J., Heymsfield, A. J., Schmitt, C., and Wilson, J. C.: Ice supersaturations exceeding 100% at the cold tropical tropopause: Implications for cirrus formation and dehydration, *Atmos. Chem. Phys.*, 5, 851–862, 2005,
<http://www.atmos-chem-phys.net/5/851/2005/>.

Kärcher, B. and Koop, T.: The role of organic aerosols in homogeneous ice formation, *Atmos. Chem. Phys.*, 5, 703–714, 2005,
<http://www.atmos-chem-phys.net/5/703/2005/>.

Koop, T., Ng, H. P., Molina, L. T., and Molina, M. J.: A new optical technique to study aerosol phase transitions: The nucleation of ice from h₂so₄ aerosols, *J. Phys. Chem. A*, 102, 8924–8931, 1998.

Koop, T., Bertram, A. K., Molina, L. T., and Molina, M. J.: Phase transitions in aqueous nh₄hso₄ solutions, *J. Phys. Chem. A*, 103, 9042–9048, 1999.

Koop, T., Luo, B. P., Tsias, A., and Peter, T.: Water activity as the determinant for homogeneous ice nucleation in aqueous solutions, *Nature*, 406, 611–614, 2000.

Koop, T.: Homogeneous ice nucleation in water and aqueous solutions, *Z. Phys. Chem.*, 218, 1231–1258, 2004.

Levien, B. J.: A physicochemical study of aqueous citric acid solutions, *J. Phys. Chem.*, 59, 640–644, 1955.

Liou, K.-T.: Influence of cirrus clouds on weather and climate processes: A global perspective, *Mon. Weather Rev.*, 114, 1167–1199, 1986.

Maffia, M. C. and Meirelles, J. A.: Water activity and ph in aqueous polycarboxylic acid systems, *J. Chem. Eng. Data*, 46, 582–587, 2001.

Maltini, E., Anese, M., and Shtylla, I.: State diagrams of some organic acid-water systems of

**Inhibition of ice
crystallisation**

B. J. Murray

Title Page

Abstract

Introduction

Conclusions

References

Tables

Figures

◀

▶

◀

▶

Back

Close

Full Screen / Esc

Printer-friendly Version

Interactive Discussion



interest in food, *Cryo-Lett.*, 18, 263–268, 1997.

McFiggans, G., Alfarra, M. R., Allan, J., Bower, K., Coe, H., Cubison, M., Topping, D., Williams, P., Decesari, S., Facchini, C., and Fuzzi, S.: Simplification of the representation of the organic component of atmospheric particulates, *Faraday Discuss.*, 130, 341–362, 2005.

Möhler, O., Linke, C., Saathoff, H., Schnaiter, M., Wagner, R., Mangold, A., Kramer, M., and Schurath, U.: Ice nucleation on flame soot aerosol of different organic carbon content, *Meteorol. Z.*, 14, 477–484, 2005.

Murphy, D. M., Thomson, D. S., and Mahoney, T. M. J.: In situ measurements of organics, meteoritic material, mercury, and other elements in aerosols at 5 to 19 kilometers, *Science*, 282, 1664–1669, 1998.

Murphy, D. M. and Koop, T.: Review of the vapour pressures of ice and supercooled water for atmospheric applications, *Q. J. Roy. Meteorol. Soc.*, 131, 1539–1565, 2005.

Murphy, D. M., Cziczo, D. J., Froyd, K. D., Hudson, P. K., Matthew, B. M., Middlebrook, A. M., Peltier, R. E., Sullivan, A., Thomson, D. S., and Weber, R. J.: Single-particle mass spectrometry of tropospheric aerosol particles, *J. Geophys. Res.-Atmos.*, 111, D23S32, doi:10.1029/2006JD007340, 2006.

Murray, B. J., Knopf, D. A., and Bertram, A. K.: The formation of cubic ice under conditions relevant to earth's atmosphere, *Nature*, 434, 202–205, 2005.

Murray, B. J. and Bertram, A. K.: Formation and stability of cubic ice in water droplets, *Phys. Chem. Chem. Phys.*, 8, 186–192, 2006.

Murray, B. J. and Bertram, A. K.: Laboratory studies of the formation of cubic ice in aqueous droplets, in: *Physics and chemistry of ice*, edited by: Kuhs, W. F., The Royal Society of Chemistry, Cambridge, 417–426, 2007a.

Murray, B. J. and Bertram, A. K.: Strong dependence of cubic ice formation on droplet ammonium to sulfate ratio, *Geophys. Res. Lett.*, 34, L16810, doi:10.1029/2007GL030471, 2007b.

Murray, B. J.: Enhanced formation of cubic ice in aqueous organic acid droplets, *Environ. Res. Lett.*, in press, 2008.

Murray, B. J. and Bertram, A. K.: Inhibition of solute crystallisation in aqueous $H^+ - NH_4^+ - SO_4^{2-} - H_2O$ droplets *Phys. Chem. Chem. Phys.*, in press, doi:10.1039/B802216J, 2008.

Peng, C., Chan, M. N., and Chan, C. K.: The hygroscopic properties of dicarboxylic and multifunctional acids: Measurements and unifac predictions, *Environ. Sci. Technol.*, 35, 4495–4501, 2001.

Peter, T., Marcolli, C., Spichtinger, P., Corti, T., Baker, M. B., and Koop, T.: When dry air is too

**Inhibition of ice
crystallisation**

B. J. Murray

Title Page

Abstract

Introduction

Conclusions

References

Tables

Figures

I◀

▶I

◀

▶

Back

Close

Full Screen / Esc

Printer-friendly Version

Interactive Discussion



- humid, *Science*, 314, 1399–1402, 2006.
- Prenni, A. J., DeMott, P. J., Kreidenweis, S. M., Sherman, D. E., Russell, L. M., and Ming, Y.: The effects of low molecular weight dicarboxylic acids on cloud formation, *J. Phys. Chem. A*, 105, 11 240–11 248, 2001.
- 5 Saxena, P. and Hildemann, L. M.: Water-soluble organics in atmospheric particles: A critical review of the literature and applications of thermodynamics to identify candidate compounds, *J. Atmos. Chem.*, 24, 57–109, 1996.
- Shilling, J. E., Tolbert, M. A., Toon, O. B., Jensen, E. J., Murray, B. J., and Bertram, A. K.: Measurements of the vapor pressure of cubic ice and their implications for atmospheric ice
- 10 clouds, *Geophys. Res. Lett.*, 33, L17801, doi:10.11029/2006gl026671, 2006.
- Tabazadeh, A., Djikaev, Y. S., and Reiss, H.: Surface crystallization of supercooled water in clouds, *Proc. Natl. Acad. Sci. USA*, 99, 15 873–15 878, 2002.
- Taylor, N. W.: Solubility of organic substances and of weak electrolytes in water, in: *International critical tables of numerical data, physics, chemistry and technology*, edited by: Washburn, McGraw-Hill, New York, 263, 250–270, 1926.
- 15 Wise, M. E., Garland, R. M., and Tolbert, M. A.: Ice nucleation in internally mixed ammonium sulfate/dicarboxylic acid particles, *J. Geophys. Res.-Atmos.*, 109, D19203, doi:10.1029/2003JD004313, 2004.
- Zhou, X. L., Geller, M. A., and Zhang, M. H.: Temperature fields in the tropical tropopause transition layer, *J. Climate*, 17, 2901–2908, 2004.
- Zobrist, B., Marcolli, C., Pedernera, D. A., and Koop, T.: Do atmospheric aerosols form glasses?, *Atmos. Chem. Phys.*, accepted, 2008.
- Zobrist, B., Weers, U., and Koop, T.: Ice nucleation in aqueous solutions of poly[ethylene glycol] with different molar mass, *J. Chem. Phys.*, 118, 10 254–10 261, 2003.
- 25 Zobrist, B., Marcolli, C., Koop, T., Luo, B. P., Murphy, D. M., Lohmann, U., Zardini, A. A., Krieger, U. K., Corti, T., Cziczo, D. J., Fueglistaler, S., Hudson, P. K., Thomson, D. S., and Peter, T.: Oxalic acid as a heterogeneous ice nucleus in the upper troposphere and its indirect aerosol effect, *Atmos. Chem. Phys.*, 6, 3115–3129, 2006.

Inhibition of ice crystallisation

B. J. Murray

Table A1. Literature data used to determine the relationship between a_w and citric acid solution concentration.

Temperature range/K	Concentration range/wt%	Reported parameter	Reference	Points in Fig. A1
298.13–319.33	8.94–59.51	$\rho_{\text{H}_2\text{O}}$	Apelblat et al. (1995)	Red filled square
298.15	4.99–49.48	a_w	Maffia and Meirelles (2001)	Pink filled triangle
289.15	0.00–93.89	a_w	Peng et al. (2001)	Green filled diamond
298	3.7–61.99	a_w	Levien (1955)	Blue cross (X)
260.9–273.1	0.19–47.45	T_m	Taylor (1926)	Blue hollow star
273.14–262.45	0.013–46.4	T_m	Apelblat (2003)	Orange hollow pentagon
250.7–272.2	10.83–58.21	T_m	This study	Black hollow circles

Title Page

Abstract

Introduction

Conclusions

References

Tables

Figures

I◀

▶I

◀

▶

Back

Close

Full Screen / Esc

Printer-friendly Version

Interactive Discussion



Inhibition of ice
crystallisation

B. J. Murray

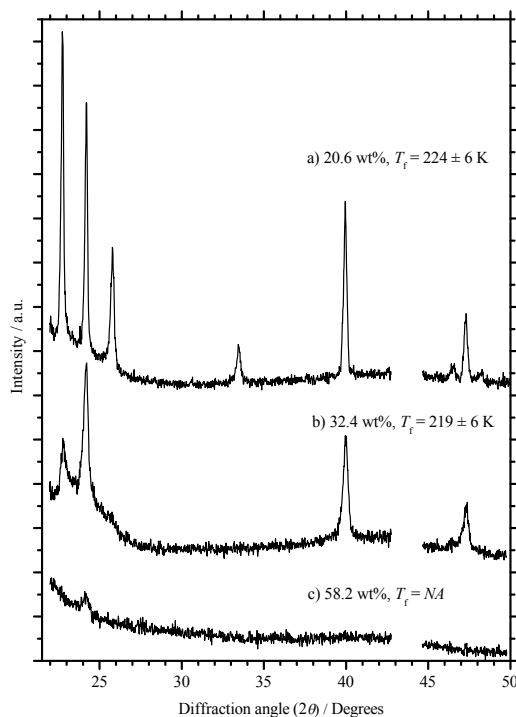


Fig. 1. Examples of diffraction patterns of citric acid solution droplets recorded at 173 K. Regions of the diffraction patterns influenced by the cell construction materials have been removed. The freezing temperature of 58.2 wt% citric acid is not available, because bulk ice did not crystallise.

[Title Page](#)[Abstract](#)[Introduction](#)[Conclusions](#)[References](#)[Tables](#)[Figures](#)[◀](#)[▶](#)[◀](#)[▶](#)[Back](#)[Close](#)[Full Screen / Esc](#)[Printer-friendly Version](#)[Interactive Discussion](#)

Inhibition of ice crystallisation

B. J. Murray

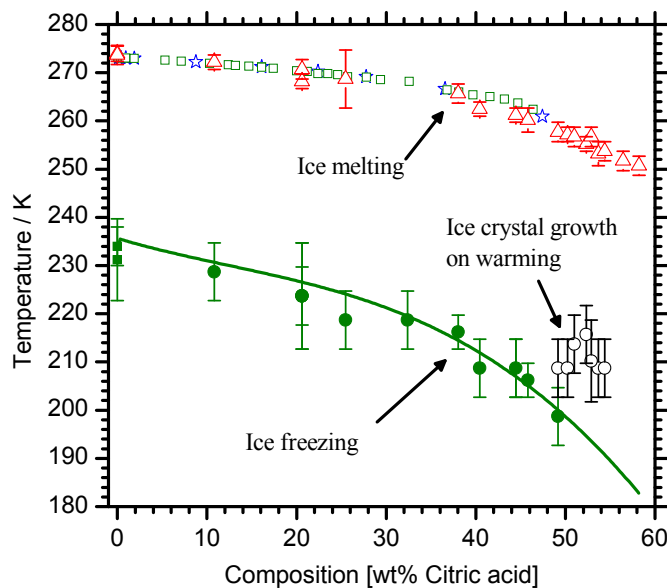


Fig. 2. State diagram for the citric acid-water system. Measurements of ice melting temperatures are plotted as red open triangles and the freezing temperatures are plotted as filled green circles. The melting temperatures are compared with literature values; green open squares (Apelblat, 2003) and blue stars (Taylor, 1926). The temperature at which ice crystallisation was observed on warming is plotted as black open circles. The solid green line is the predicted ice nucleation temperature based on the relationship between the freezing and measured melting point depressions; see Fig. 3 and the text for details.

[Title Page](#)[Abstract](#)[Introduction](#)[Conclusions](#)[References](#)[Tables](#)[Figures](#)[I◀](#)[▶I](#)[◀](#)[▶](#)[Back](#)[Close](#)[Full Screen / Esc](#)[Printer-friendly Version](#)[Interactive Discussion](#)

Inhibition of ice
crystallisation

B. J. Murray

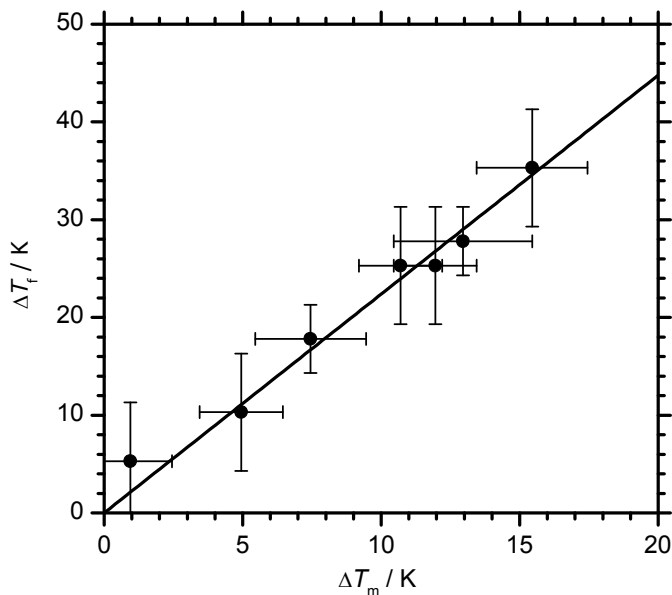


Fig. 3. The freezing temperature depression as a function of the melting point depression. See text for details. The solid line is a best fit forced through the origin (slope= $\lambda=2.24\pm 0.06$).

[Title Page](#)[Abstract](#)[Introduction](#)[Conclusions](#)[References](#)[Tables](#)[Figures](#)[I◀](#)[▶I](#)[◀](#)[▶](#)[Back](#)[Close](#)[Full Screen / Esc](#)[Printer-friendly Version](#)[Interactive Discussion](#)

Inhibition of ice crystallisation

B. J. Murray

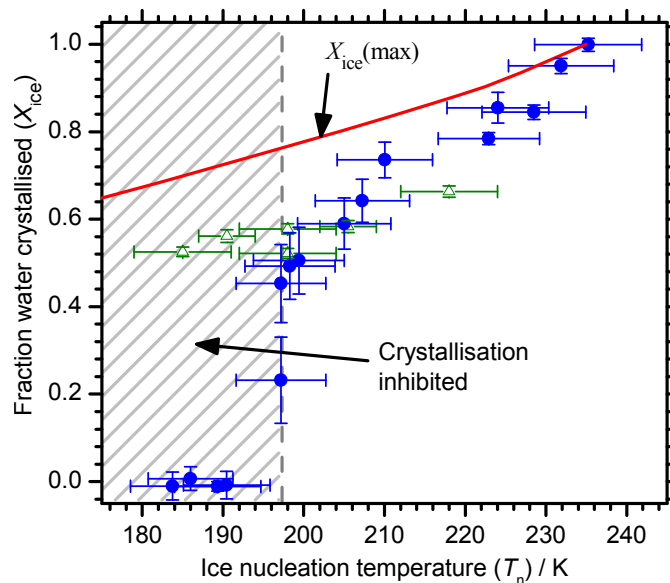


Fig. 4. The fraction of water in solution droplets which crystallised to ice (X_{ice}) when cooled to 173 K at a rate of 5 K min^{-1} , expressed as a function of ice nucleation temperature. Data for citric acid is plotted as blue filled circles. An X_{ice} value of 1 indicates all water crystallised and a value of 0 indicates none crystallised. The nucleation temperature was determined using the relationship between the ice freezing and ice melting point depression (i.e. $\Delta T_n = \lambda \Delta T_m$, where $\lambda = 2.24 \pm 0.06$, see text for details). The solid red line is the maximum X_{ice} in citric acid solution droplets; i.e. it is the X_{ice} for ice in equilibrium with an aqueous citric acid brine at 173 K assuming there are no kinetic limitations to ice crystallisation and the citric acid does not crystallise to a solid citric acid phase. X_{ice} is also plotted for ammonium bisulphate solution droplets using an identical experimental procedure (green open triangles).

[Title Page](#)[Abstract](#)[Introduction](#)[Conclusions](#)[References](#)[Tables](#)[Figures](#)[◀](#)[▶](#)[◀](#)[▶](#)[Back](#)[Close](#)[Full Screen / Esc](#)[Printer-friendly Version](#)[Interactive Discussion](#)

Inhibition of ice crystallisation

B. J. Murray

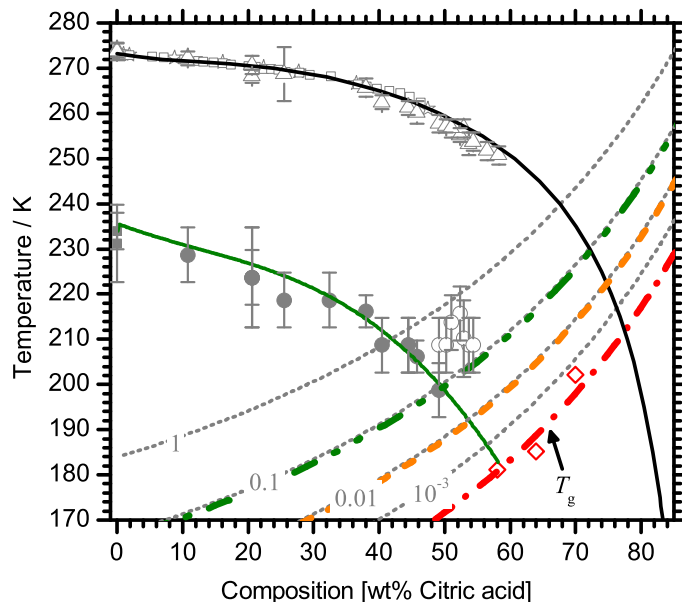


Fig. 5. State diagram, glass transition and diffusion distances for the citric acid-water system. The black solid line is an estimate of the ice-liquid equilibrium line based on water activity data; see Appendix A for details. The experimental data for melting, freezing and crystal growth on warming from Fig. 3 have been included for comparison as gray symbols. The predicted T_n line from Fig. 3 is also included as a solid green line. Literature data for the glass transition temperature measured by differential scanning calorimetry together with a parameterisation for this data are shown as red open diamonds and a dot-dashed line, respectively. The dotted gray lines are line of constant root mean square distance of water molecules in aqueous solution. The labels indicate the root mean square distance (micrometers) water molecules are expected to diffuse in 1 min. The dot-dot-dashed green line represents the approximate limiting value of $x_{\text{H}_2\text{O}}$ ($0.09 \mu\text{m}$) below which ice crystal growth is inhibited at a cooling rate of 5K min^{-1} , whereas the dashed orange line represents the $x_{\text{H}_2\text{O}}$ ($0.009 \mu\text{m}$) below which ice crystal growth is estimated to be inhibited at cooling rate of 0.5K min^{-1} .

Title Page

Abstract

Introduction

Conclusions

References

Tables

Figures

◀

▶

◀

▶

Back

Close

Full Screen / Esc

Printer-friendly Version

Interactive Discussion



Inhibition of ice
crystallisation

B. J. Murray

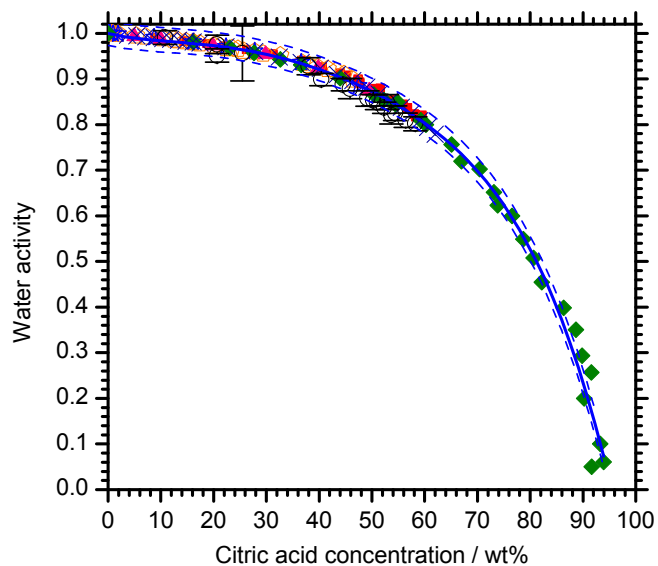


Fig. A1. Water activity data as a function of citric acid concentration. See Table A1 for sources and a key to the literature data. The solid line is a polynomial fit and the dashed lines represent 95% prediction limits.

[Title Page](#)[Abstract](#)[Introduction](#)[Conclusions](#)[References](#)[Tables](#)[Figures](#)[I◀](#)[▶I](#)[◀](#)[▶](#)[Back](#)[Close](#)[Full Screen / Esc](#)[Printer-friendly Version](#)[Interactive Discussion](#)